



Parametric analysis of the operation of nocturnal radiative cooling panels coupled with in room PCM ceiling panels

Bourdakis, Eleftherios; Kazanci, Ogun Berk; Péan, T.Q.; Olesen, Bjarne W.

Published in:
Proceedings of the 2017 ASHRAE Winter Conference

Publication date:
2017

Document Version
Peer reviewed version

[Link back to DTU Orbit](#)

Citation (APA):
Bourdakis, E., Kazanci, O. B., Péan, T. Q., & Olesen, B. W. (2017). Parametric analysis of the operation of nocturnal radiative cooling panels coupled with in room PCM ceiling panels. In Proceedings of the 2017 ASHRAE Winter Conference

General rights

Copyright and moral rights for the publications made accessible in the public portal are retained by the authors and/or other copyright owners and it is a condition of accessing publications that users recognise and abide by the legal requirements associated with these rights.

- Users may download and print one copy of any publication from the public portal for the purpose of private study or research.
- You may not further distribute the material or use it for any profit-making activity or commercial gain
- You may freely distribute the URL identifying the publication in the public portal

If you believe that this document breaches copyright please contact us providing details, and we will remove access to the work immediately and investigate your claim.

Parametric Analysis of the Operation of Nocturnal Radiative Cooling Panels Coupled with in Room PCM Ceiling Panels

E. Bourdakis

Student member ASHRAE

O.B. Kazanci

Student Member ASHRAE

T.Q. Péan

B. W. Olesen, PhD

Fellow ASHRAE

ABSTRACT

The scope of this parametric simulation study was to identify the optimal combination of set-points for different parameters of a radiant PCM ceiling panels cooling system that will result in the best indoor thermal environment with the least possible energy use. The results showed that for each parameter examined, a different set-point value was optimal for the thermal environment than the value that was optimal for the reduction of energy use. Therefore, two additional simulations were run, one with the combination of set-point values that resulted in the improvement of the thermal environment and one with the set-point values resulting in the reduction of energy use. In the first case, the temperature was within the range of Category III of EN 15251 (23 – 26°C, 73.4 – 78.8°F) for 83.5% of the occupancy time, while in the second case it was within Category III for 39.4%. In the first simulation, the energy usage of the pumps and the heat pump was 178 kWh, 608 kBtu, while for the second one it was 36 kWh, 121 kBtu. It was concluded that the optimal combination of set-point values to provide the most comfortable thermal environment was to activate the pump circulating water to the PCM no earlier than 03:00 and get activated when the temperature in the storage tank was below 21°C, 69.8°F, activate the heat pump no earlier than 05:00 and get activated when the temperature in the storage tank was below 15°C, 59°F, and lastly have a temperature difference between the output of the solar panels and the temperature in the middle of the storage tanks of 5 K, 9°F.

INTRODUCTION

As HVAC systems advance, their operation and control system becomes increasingly complicated, consisting of multiple conditions and parameters, which interact with each other. In order to optimize the operation of a control system, the ideal combination of set-points for these parameters needs to be realized, aiming at providing an acceptable indoor environment, as this is defined by the standards, and at the same time reducing the energy use as much as possible. The operation optimization of the controller of radiant heating and cooling systems has been the subject of several studies, both simulations and experimental.

Sourbron and Helsen (2013) studied the impact of using different temperature (air, operative, surface and core temperature) for controlling a Thermo Active Building System (TABS) and different setpoint values for these parameters. They concluded that the controller settings, apart from the indoor thermal environment and the energy use, affect considerably also the required power of the heating and cooling source. In addition to that, inappropriate control settings resulted in switching between heating and cooling mode during the same day, resulting in a significant increase of the energy used by the radiant system.

Tödli et al. (2007) and Gwerder et al. (2008) studied the coupling of TABS control with building automation and developed a tool for dimensioning the TABS using the “Unknown-But-Bounded” method. With this method they were able to verify the system’s applicability for a given situation, determine the maximum heating/cooling

E. Bourdakis is a Ph.D. candidate in the ICIEE, Technical University of Denmark, Denmark. **O.B. Kazanci** is a PhD candidate. in the ICIEE, Technical University of Denmark, Denmark. **T.Q. Péan** is a PhD student at the Polytechnic University of Catalonia, Spain. **B.W. Olesen** is a Professor in the ICIEE, Technical University of Denmark, Denmark

capacity and maintain the thermal comfort, provided that the heat gains were within the predefined range.

Lim et al. (2006) studied radiant floor cooling systems in Korean residential buildings regarding the possibility of condensation occurrence and thermal comfort due to the Korean tradition of sitting on the floor. They concluded that controlling the room air temperature by adjusting the supply water temperature and having a constant water flow provided better thermal environment than controlling with a variable water flow. Regarding condensation, they suggested that the water supply temperature should be adjusted based on the room dew point temperature.

In a different study, Lim et al. (2014), developed an operational guideline for TABS, based on heating and cooling load characteristics of a specific campus building in Seoul, Korea. Furthermore, they found that although the radiant system was able to deal with most of the heating load, it was able to remove less than 50% of the cooling loads due to the limitations caused by the risk of forming condensation on the radiant surface.

In the present simulation study, the coupling of solar panels with in room Phase Change Material (PCM) ceiling panels for cooling an office room was examined during the summer (cooling) period of Copenhagen, Denmark. The solar panels were utilized to produce cold water through nocturnal radiative cooling which was then used to discharge the PCM panels in the room. The purpose of this parametric study was to identify the optimal combination of set-point values that will result in providing the ideal indoor thermal environment. The simulation model that was used, has already been validated and tested under different climatic conditions (Bourdakis et al. 2015; 2016a).

METHODOLOGY

The model was created using commercially available software, to simulate an office room located in Copenhagen, Denmark. The simulation period was from the 1st of May until the 30th of September which is considered the cooling period in Denmark, using the corresponding IWEC weather file. The floor dimensions were 5.4 m X 4.2 m (17.7 ft X 13.8 ft) corresponding to 22.7 m² (244.3 ft²), while the total height was 3 m (9.8 ft). At 2.5 m (8.2 ft) above the floor PCM panels were installed forming a suspended ceiling as it can be seen in Figure 1. Outside air was supplied to the office from the plenum formed between the suspended ceiling panels and the roof of the office. The office was assumed to be in an intermediate floor of an office building and the external wall of the office was facing south. Therefore, the three internal walls, the roof and the floor were assumed to be adjacent to office rooms with identical thermal conditions, so no heat exchange occurred from these surfaces. The U-value of the external wall was 0.3 W/m²K (0.1 Btu/ft².h.°F) while the internal surfaces had a U-value of 4.9 W/m²K (0.9 Btu/ft².h.°F). On the external wall there was a 3 m² (32.3 ft²) window with a U-value of 1.4 W/m²K (0.2 Btu/ft².h.°F) and a g-value of 0.59. The heat gains of the office consisted of two occupants at sedentary activity level (1.2 Met), the corresponding office equipment and lighting which in total was 540 W (1843 Btu/h) corresponding to 23.8 W/m² (7.5 Btu/h.ft²). The heat gains were activated during typical office hours, namely from 9:00 to 17:00.

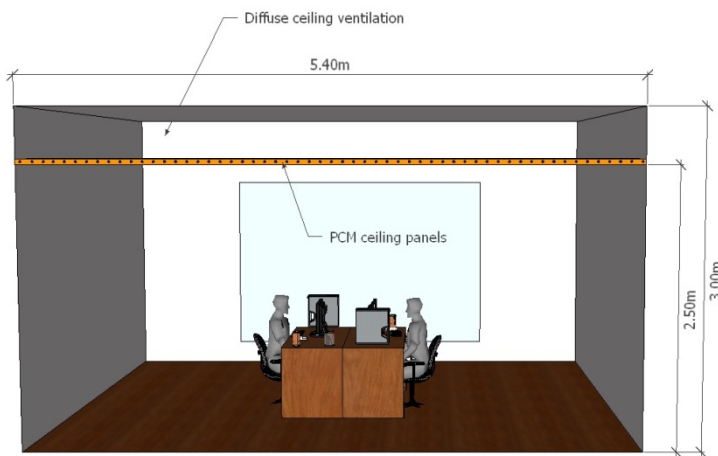


Figure 1. Vertical cross-section of the simulated office room

The PCM panels covered 18.8 m² (201.8 ft²) of the total ceiling surface and the panel thickness was 25 mm (0.082 ft). The PCM density was 1217 kg/m³ (76 lb/ft³) while the latent enthalpy was 28.7 kJ/kg (12.3 Btu/lb). The phase change temperature range of the PCM was 21 – 25°C (70°F – 77°F). The PCM ceiling panels had embedded pipes for water circulation to discharge the PCM. The external diameter of the pipes was 8 mm (0.026 ft), the pipe thickness was 1 mm, the pipe spacing was 85 mm (0.279 ft). and the water flow rate was 150 kg/h (331 lb/h). The ventilation system was sized based on EN 15251 (DS/EN 2007) for providing outside air and removing pollutants, which resulted in an air flow rate of 30 L/s (63.6 ft³/min) corresponding to 1.9 ACH. The ventilation was operating during the occupancy period, namely 09:00 – 17:00 and the air supply temperature was 18.5°C (65.3°F).

Three PhotoVoltaic/Thermal (PV/T) panels and an unglazed solar collector were installed for providing electricity, hot and cold water to the office. The cold water would be utilized to discharge the PCM. The solar collectors were facing south at a tilt angle of 45°. The total surface of the PV/T panels was 3.9 m² (42 ft²) while for the unglazed solar collector was 2.4 m² (25.8 ft²). The water flow rate in the solar panels was 100 kg/h (220 lb/h) and was split in 62 kg/h (136 lb/h) for the PV/T panels and 38 kg/h (84 lb/h) for the unglazed solar collector in order to ensure the same water flow rate per m² for the two types of solar collectors. The emissivity of the absorber plate of the unglazed solar collector was 0.91 while for the PV/Ts was 0.89. The plate absorptance of the collectors was 0.95. The PV/T panels had 15 water tubes with an inner diameter of 18 mm (0.06 ft) and a thickness of 1 mm (0.003 ft).

Two tanks were used to store the hot water (HWT) and the cold water (CWT) output of the solar collectors. Between the solar collectors and the storage tanks a plate heat exchanger was used due to the different pressure settings of the tanks and the solar collectors. A schematic drawing of the hydronic system is shown in Figure 2.

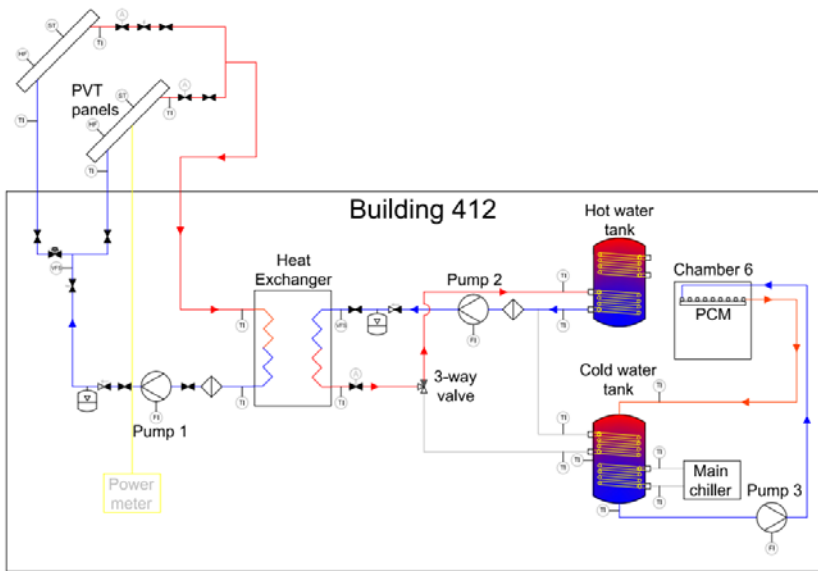


Figure 2. Schematic drawing of the hydronic system

After the heat exchanger a 3-way valve was installed to direct the water either towards the CWT or the HWT. The direction of the water was determined automatically based on the following conditions:

$$\text{If } T_{PV/T} - T_{HWT} > \Delta T \text{ then water directed towards HWT} \quad (1)$$

$$\text{If } T_{CWT} - T_{PV/T} > \Delta T \text{ then water directed towards CWT} \quad (2)$$

where $T_{PV/T}$ is the water temperature exiting the PV/T panels, T_{HWT} is the temperature in the middle of the HWT and T_{CWT} is the temperature in the middle of the CWT. If neither of the two conditions was met, then pump 2 (see Figure 2) was switched off. The ΔT was one of the examined parameters, and the values used were 1 K, 2 K, 3 K, 4 K and 5 K (1.8°F, 3.6°F, 5.4°F, 7.2°F and 9°F, respectively). The CWT had two internal spiral heat exchangers. The upper one was connected to the heat exchanger, while the lower one was connected to an air-to-water heat pump (AWHP) as shown in Figure 2. The AWHP was used as a supporting system for providing cold water when the production from nocturnal radiative cooling was not sufficient. The AWHP had a seasonal COP of 5.4 (18.4 EER).

The hot water was not utilized, e.g. through a tapping schedule and the tank was used only to store hot water in order to reduce the surface temperature of the PV/T panels. In this way the efficiency of the PV/T panels in terms of electricity production would be increased.

The examined parameters were the set-point temperature and the starting time for activating Pump 3 circulating water to PCM panels, the set-point temperature and the starting time for activating the AWHP, and, the temperature difference between the outlet temperature of the solar panels and the water temperature in the middle of the storage tanks. For both Pump 3 and the AWHP, the setpoint temperature was the temperature in the middle of the CWT. The values that were examined for each parameter are shown in Table 1, and the values that were used when examining a different parameter are highlighted in bold. Since the setpoints for activating Pump 3 and the AWHP are closely related, all the possible combinations of these two parameters were simulated.

Table 1. Setpoint values for examined parameters

AWHP starting time, hh:mm	CWT temperature to activate the AWHP, K (°F)	Pump 3 starting time, hh:mm	CWT temperature to activate Pump 3, K (°F)	Panels – Tanks ΔT , K (°F)
03:00	15 (59)	03:00	15 (59)	1 (1.8)
04:00	16 (60.8)	04:00	16 (60.8)	2 (3.6)
05:00	17 (62.6)	05:00	17 (62.6)	3 (5.4)
06:00	18 (64.4)	06:00	18 (64.4)	4 (7.2)
07:00	19 (66.2)	07:00	19 (66.2)	5 (9)
	20 (68)		20 (68)	
	21 (69.8)		21 (69.8)	

The examined parameters will be evaluated in terms of the indoor thermal environment of the office and the energy required for the operation of the pumps and the AWHP. The thermal environment will be assessed in terms of percentage of occupancy time that the operative temperature was within the range of Category III of EN 15251 (DS/EN 2007), which is 22 – 27°C (71.6°F – 80.6°F). The PCM panels will be assessed in terms of cooling energy removed by the PCM ceiling panels and the utilization factor of the PCM, namely the percentage of PCM quantity being discharged or charged at the beginning or the end of the occupancy period respectively.

RESULTS

In the following tables, the results from each set of simulations are presented. The optimal value for each output is highlighted in bold. The results from the simulations in which the starting time of the operation of the AWHP was examined, are shown in Table 2. The calculations of the energy use of the pumps and the AWHP is based on the calculations done previously by Bourdakis et al. (2016a, 2016b).

Table 2. Results from the AWHP starting time simulations

AWHP starting time, hh:mm	Percentage of occupancy time in Category III, %	Pumps energy usage, kWh (kBtu)	AWHP energy usage, kWh (kBtu)	Energy removed by the PCM, kWh (kBtu)	Percentage of PCM discharged at 09:00, %	Percentage of PCM charged at 17:00, %
03:00	65.6	48 (162)	74 (253)	50 (169)	84.2	82.2
04:00	65.6	48 (162)	74 (251)	50 (169)	84.2	82.1
05:00	65.9	48 (162)	72 (247)	49 (168)	83.7	82.1
06:00	64.4	47 (161)	66 (226)	48 (165)	82.5	82.5
07:00	62.3	46 (160)	55 (187)	46 (157)	79.4	83.2

In Table 3 the results from the simulations in which the starting time of the operation of Pump 3 was examined, are presented.

Table 3. Results from the Pump 3 starting time simulations

Pump 3 starting time, hh:mm	Percentage of occupancy time in Category III, %	Pumps energy usage, kWh (kBtu)	AWHP energy usage, kWh (kBtu)	Energy removed by the PCM, kWh (kBtu)	Percentage of PCM discharged at 09:00, %	Percentage of PCM charged at 17:00, %
03:00	70.4	52 (176)	99 (337)	59 (200)	94.7	77.9
04:00	68.5	50 (170)	88 (301)	54 (185)	90.7	80.2
05:00	65.9	48 (162)	72 (247)	49 (169)	83.7	82.1
06:00	62.3	45 (153)	52 (177)	44 (150)	74.8	83.5
07:00	59.9	43 (146)	32 (110)	39 (132)	65.1	84.1

The results from the simulations in which the temperature difference of the output of the solar panels and the temperature in the middle of the storage was examined, are shown in Table 4.

Table 4. Results from the Panels – Tanks ΔT simulations

Panels – Tanks ΔT , K (°F)	Percentage of occupancy time in Category III, %	Pumps energy usage, kWh (kBtu)	AWHP energy usage, kWh (kBtu)	Energy removed by the PCM, kWh (kBtu)	Percentage of PCM discharged at 09:00, %	Percentage of PCM charged at 17:00, %
1 (1.8)	65.9	48 (162)	72 (246)	49 (169)	83.7	82.1
2 (3.6)	65.8	47 (161)	73 (247)	49 (169)	83.7	82.2
3 (5.4)	65.8	47 (159)	73 (248)	49 (169)	83.7	82.1
4 (7.2)	65.8	46 (157)	73 (250)	48 (168)	83.7	82.2
5 (9)	65.6	45 (156)	74 (253)	48 (168)	83.5	82.2

In Figure 3 the percentage of occupancy period outside the range of Category III of Standard EN 15251 vs the energy usage of the pumps and the AWHP in terms of kWh/m² is presented, for the cases of AWHP and Pump 3 operation starting time and the temperature difference between the output of the solar panels and the temperature in the middle of the storage tanks.

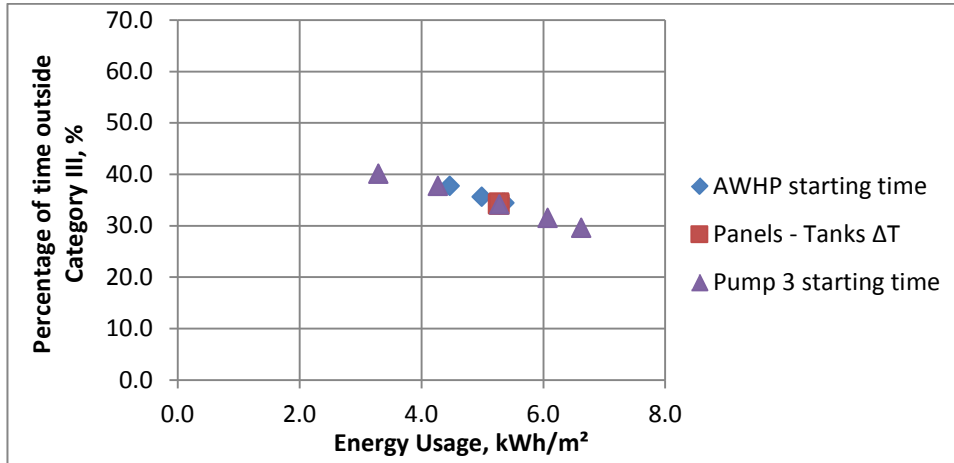


Figure 3 Percentage of time outside Category III vs energy use

In Figure 4 the percentage of occupancy period outside the range of Category III of Standard EN 15251 vs the energy usage of the pumps and the AWHP in terms of kWh/m² is presented for the cases of set-point values for the activation of the AWHP and Pump 3.

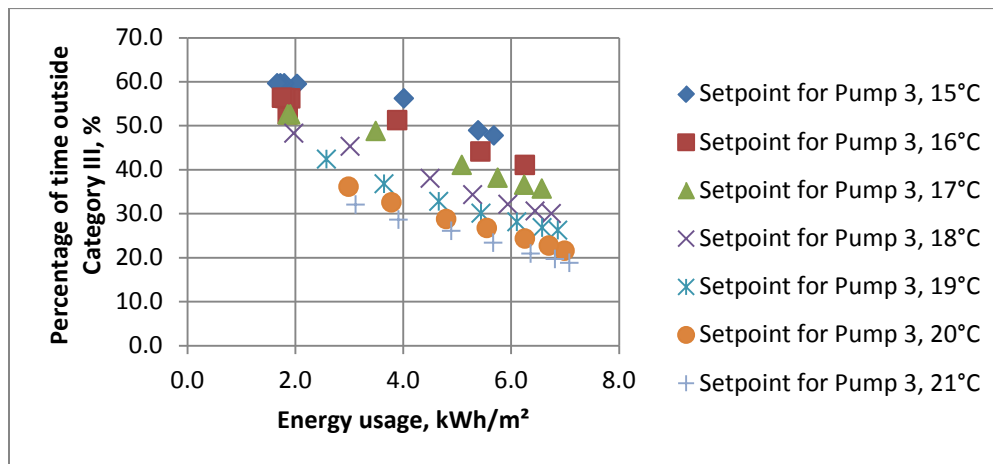


Figure 4 Percentage of time outside Category III vs energy use for AWHP and Pump 3 setpoint simulations

DISCUSSION

From Table 2 it can be seen that the starting time of the operation of the AWHP did not have a clear impact on the indoor thermal environment, since the higher percentage of occupancy time occurred when the AWHP was activated on earlier than 05:00. On the other hand, as it can be seen from Table 3, the earlier Pump 3 is starting to operate, the higher the percentage of occupancy time within Category III of EN 15251, as it was expected. For both the AWHP and Pump 3, the later the operation starts, the lower the energy usage of the pumps and the AWHP is. The impact of the starting time of Pump 3 is significantly higher for the energy usage of pumps and AWHP compared to the starting time setpoint of the AWHP itself. The reason is that if Pump 3 is activated earlier than the AWHP, the temperature in the middle of the CWT will increase and then the AWHP will be required to operate for more time once it gets activated. On the other hand, if the AWHP is activated prior to Pump 3, the temperature in the middle of the CWT will not increase until Pump 3 is activated, and the AWHP will only need to operate if nocturnal radiative cooling is not enough for cooling down the water in the CWT. That is why the energy usage of AWHP is increased only by 1.9 kWh, 6500 Btu when the start of the AWHP operation changes from 05:00 to 03:00, as it is shown in

Table 2, while for the same time change of the operation of Pump 3 the increase in the energy use is 26.4 kWh, 90000 Btu. Regarding the cooling energy removed by the PCM, the impact of the starting time set-point of the AWHP is insignificant (ranges from 46 kWh to 50 kWh) compared to the impact of the starting time setpoint of Pump 3 (ranges from 38 kWh to 59 kWh). For both cases, the earlier the operation starts, the higher percentage of PCM is discharged before the start of the occupancy period and the lower percentage is utilized at the end of it. As before, the impact is higher in the case of the activation time of Pump 3.

From the results reported in Table 4, it can be seen that no significant changes were observed in any of the examined outputs. For that reason, further analysis was required for this parameter. Therefore, it was examined in terms of activation sensitivity, namely how many times Pump 2 was activated/deactivated on average during a day. In Table 5 the average times Pump 2 was activated and deactivated per day are shown.

Table 5. Pump 2 activation sensitivity

Panels – Tanks ΔT , K ($^{\circ}$ F)	1 (1.8)	2 (3.6)	3 (5.4)	4 (7.2)	5 (9)
Activation/deactivation times per day	16	12	8	6	4

From Table 5 it can be seen that the higher the ΔT between the water temperature exiting the solar panels and the middle of the storage tanks, the lower the number the pumps is activated or deactivated during a day, ensuring a more stable operation of the pump.

As it can be seen in Figure 3 and Figure 4, there is a clear trend for all the examined parameters; the lower the percentage of occupancy period outside the range of Category III the higher the energy usage. As mentioned before, the only exception is the ΔT between the output of the solar panels and the middle of the storage tanks, for which all the points almost coincide, as it is shown in Figure 3. For that reason, two more simulations were run, with the combination of settings that contributed the most in energy savings and providing the optimal indoor thermal environment. Since the ΔT between the output of the solar panels and the middle of the storage tanks had no impact either in the energy savings of the system or the provided indoor thermal environment, the ΔT of 5 $^{\circ}$ C (9 $^{\circ}$ F) was chosen for both simulations since it gave the most stable operation for Pump 2. Table 6 shows the set-points used in the last two simulations.

Table 6. Setpoint values for examined parameters for optimized simulations

	AWHP starting time, hh:mm	CWT temperature to activate the AWHP, K ($^{\circ}$ F)	Pump 3 starting time, hh:mm	CWT temperature to activate Pump 3, K ($^{\circ}$ F)	Panels- Tanks ΔT , K ($^{\circ}$ F)
Energy savings simulation	07:00	21 (69.8)	07:00	15 (59)	5 (9)
Indoor thermal environment simulation	05:00	15 (59)	03:00	21 (69.8)	5 (9)

In Table 7 the results from the two optimized simulations are presented. By comparing these results with the results shown in Table 2, Table 3 and Table 4, it can be seen that the simulation focused on energy savings had significantly lower energy usage for the pumps and the AWHP, but with a considerable compromise on the indoor thermal environment. On the other hand, the last simulation provided the best indoor thermal environment, 83.5% of occupancy time within the range of Category III, but with the higher energy usage observed among all the

simulations, namely 178 kWh (198 kBtu).

Table 7. Results from the optimized simulations

	Percentage of occupancy time in Category III, %	Pumps energy usage, kWh (kBtu)	AWHP energy usage, kWh (kBtu)	Energy removed by the PCM, kWh (kBtu)	Percentage of PCM discharged at 09:00, %	Percentage of PCM charged at 17:00, %
Energy savings simulation	39.4	34 (116)	2 (5)	16 (56)	53.4	91.1
Indoor thermal environment simulation	83.5	58 (198)	120 (410)	69 (235)	97.3	43.4

CONCLUSION

All the examined parameters had inverse results in terms of energy use and indoor thermal environment, namely the better the indoor thermal environment provided, the higher the energy use of pumps and the heat pump. The only exception was the ΔT between the water temperature exiting the solar panels and the temperature in the middle of the storage tanks. For this ΔT , the highest examined value (5K, 9°F) performed the best by having the most stable operation. Based on that, it was concluded that when an output of a condition is based on a temperature difference, the set-point value should be carefully decided in order to avoid continuous activation/deactivation of the pump or the heat pump, that could possibly damage it. The ideal combinations of setpoints for providing the best indoor thermal environment and minimizing the energy use were identified. The impact of the starting time of the operation of the AWHP was less significant than the starting time of the operation of Pump 3 in terms of indoor thermal comfort and energy.

REFERENCES

- Bourdakis, E., Olesen, B. W., & Grossule, F. (2015). Night time cooling by ventilation or night sky radiation combined with in - room radiant cooling panels including Phase Change Materials. In 36 Air Infiltration Ventilation Centre Conference.
- Bourdakis, E., Kazanci, O. B., Grossule, F., & Olesen, B. W. (2016a). Simulation Study of Discharging PCM Ceiling Panels through Night-time Radiative Cooling. In ASHRAE Transactions.
- Bourdakis, E., Péan, T., Gennari, L., & Olesen, B. W. (2016b). Daytime space cooling with Phase Change Material (PCM) ceiling panels discharged using rooftop PV / T panels and night-time ventilation. *Science and Technology for the Built Environment*, 1–9.
- DS/EN. (2007). DS/EN 15251:2007 Indoor environment input parameters for design and assessment of energy performance of buildings addressing indoor air quality, thermal environment, lighting and acoustics.
- Gwerder, M., Lehmann, B., Tödli, J., Dorer, V., & Renggli, F. (2008). Control of thermally-activated building systems (TABS). *Applied Energy*, 85(7), 565–581.
- Lim, J. H., Jo, J. H., Kim, Y. Y., Yeo, M. S., & Kim, K. W. (2006). Application of the control methods for radiant floor cooling system in residential buildings. *Building and Environment*, 41(1), 60–73.
- Lim, J. H., Song, J. H., & Song, S. Y. (2014). Development of operational guidelines for thermally activated building system according to heating and cooling load characteristics. *Applied Energy*, 126, 123–135.
- Sourbron, M., & Helsen, L. (2013). Sensitivity analysis of feedback control for concrete core activation and impact on installed thermal production power. *Journal of Building Performance Simulation*, 7(5), 1–17.
- Tödli, J., Gwerder, M., Lehmann, B., Renggli, F., & Dorer, V. (2007). Integrated Design Of Thermally Activated Building Systems And Of Their Control. In CLIMA 2007.